Virchows Archiv (1995) 426:141–148

ORIGINAL ARTICLE

J. Alroy · K. Knowles · S. H. Schelling · E. M. Kaye
A. E. Rosenberg

Retarded bone formation in G_{M1}-gangliosidosis: a study of the infantile form and comparison with two canine models

Received: 5 August 1994 / Accepted: 15 November 1994

Abstract The development of skeletal lesions in two canine models of G_{M1}-gangliosidosis, English springer spaniels and Portuguese water dogs, has been studied and compared to osseous abnormalities in a child with the infantile form of the disease. In the canine models, skeletal dysplasia was progressive. Lesions were noted at 2 months of age and characterized by retarded endochondral ossification and osteoporosis. Older puppies had focal cartilage necrosis within lumbar vertebral epiphyses. At the cellular level, lesions were characterized by chondrocytic hypertrohy and lysosomal accumulation of storage compounds. Our studies illustrate that the skeletal lesions in both canine models are similar to those in a child with G_{M1}-gangliosidosis. Furthermore, we proposed that the abnormal storage of partially degraded compounds in affected chondrocytes might explain, at least in part, the retarded bone formation noted in patients with G_{M1}-gangliosidosis.

Key words Retarded bone formation · G_{M1}-gangliosidosis · Canine model

Introduction

Lysosomal storage disorders are a large group of hereditary diseases resulting from deficient activity of one or more lysosomal enzymes. Many of the lysosomal storage disorders are associated with malformations of the skeleton. The skeletal lesions observed in humans and animals with lysosomal storage disorders have been recently reviewed [1]. Amongst the abnormalities noted were short stature, dysmorphic facial features, limitation of joint mobility, kyphoscoliosis, atlantoaxial dislocation, osteopaenia, osteonecrosis and osteosclerosis [1, 5, 20, 23, 24, 29, 33, 34]. Although radiographic findings in many lysosomal disorders are relatively distinct and can be useful in establishing the diagnosis [20, 29, 33, 34], there are limited morphological descriptions of either cartilaginous or bony lesions from case reports of individuals afflicted with these disorders [17, 27, 28, 31].

Animal models contribute to our understanding of lysosomal storage diseases [2]. The development of skeletal lesions in cats with mucopolysaccharidosis (MPS)-VI has been assessed radiographically [15]. However, only brief morphological descriptions of the skeletal lesions in feline models for MPS-I and MPS-VI [10, 11], and canine and murine models for MPS-VII [12, 36] have been reported. The absence of systematic morphological evaluations of the skeletal lesions in any of these disorders has precluded an understanding of the mechanisms by which lysosomal storage disease-associated skeletal dysplasias develop.

G_{M1}-gangliosidosis is a lysosomal storage disease caused by deficient activity of the lysosomal enzyme acid β-galactosidase. This results in lysosomal accumulation of glycolipids, keratan sulfate and oligosaccharides with a non-reducing terminal β-galactosidic linkage in multiple tissues and various cell types. The infantile form (type 1) of the disease is associated with severe skeletal changes [24]. Skeletal changes have been observed in two canine models of G_{M1}-gangliosidosis [3]. This report describes the evolution of skeletal lesions in English springer spaniels (ESS) and Protuguese water dogs (PWD) with G_{M1}-gangliosidosis and compares their skeletal abnormalities with those observed in a child with the infantile form of G_{M1}-gangliosidosis.

J. Alroy (✉) · S. Schelling
Department of Pathology, Tufts University School of Medicine and Veterinary Medicine,
136 Harrison Avenue, Boston, MA 02111, USA

K. Knowles
Department of Medicine, Tufts University School of Veterinary Medicine, Grafton, Massachusetts, USA

E. Kaye
Division of Pediatric Neurology, Tufts University School of Medicine, Boston, Massachusetts, USA

A. Rosenberg
Department of Pathology, Massachusetts General Hospital, Boston, Massachusetts, USA

Materials and methods

We studied 11 affected PWD dogs, 3 affected ESS dogs, corresponding breed, age- and sex-matched control dogs, and an affected child. Diagnosis in the affected puppies was established at 7 weeks of age; in the child, it was made at 6 weeks of age. Assays of acid β-galactosidase activity in white blood cells and placentas were used to confirm the diagnosis in affected puppies [3] and in leukocytes of the child [30]. The determinations were performed in duplicate using synthetic florigenic 4-methylumbelliferyl-galactoside as substrate, and the values were compared with those obtained from their siblings, with unrelated ESS and PWD dogs and with control human patients. The dogs had radiographic examinations at 2 months of age and every 3 months thereafter. Affected dogs and age-matched controls were killed at 2–5, 7, 8 and 9 months of age by an intravenous injection of sodium pentobarbital and necropsied. Tissue samples from each dog were obtained for light and electron microscopic evaluation. The child died at 15 months of age and was immediately autopsied. Tissue samples for light and electron microscopy were collected.

For light microscopy the following specimens were collected from the puppies: proximal and distal femoral and humeral epiphyses, proximal parts of radii, ulnae, tibiae and fibulae, third and fourth lumbar vertebrae, and the cartilage of the costocondral junction. From the child the femur, the third lumbar vertebra and cartilage from the costochondral junction were obtained. Bones were hemisected on a band saw, fixed in 10% buffered formalin, demineralized in 5% nitric acid and embedded in paraffin. Tissue blocks were sectioned at 5 μm and stained with haematoxylin and eosin and safranin-O. To overcome alteration of glycoconjugates produced by demineralization, lectin-staining was performed only on the cartilage specimens from the costochondral junction. Table 1 lists the 11 different lectins used, their acronyms, the lectin concentrations used, their major sugar specificity, and corresponding sugars used to inhibit their bindings. We used biotinylated lectins and avidin-biotin-peroxidase complex (ABC) to demonstrate the storage compound/s in chondrocytes. A detailed protocol for lectin staining has been reported earlier [3]. In addition, cartilage from the castochondral junction was stained for the presence of S-100 protein and neuron specific enolase. We used biotinylated rabbit anti S-100 protein and neuron specific enolase (Dako Corp., Calif., USA) and ABC.

For electron microscopic studies samples of cartilage were obtained from affected and normal control puppies and from the affected child. They were fixed in Trump's fixative in cacodylate buffer, pH 7.2, post-fixed in 1% osmium tetroxide in 0.1 M cacodylate buffer, pH 7.4, dehydrated through graded ethanol solutions, and embedded in Embed-812 epoxy resin. For orientation 1 μm thick sections were stained with toluidine blue. Sections 50 nm thin were cut, stained with uranyl acetate and lead citrate and photographed with a Philips EM 201 electron microscope.

Results

Radiological and necropsy findings

Radiographic evaluation of the vertebral columns revealed irregular intervertebral disk spaces in affected 2-month-old ESS and PWD puppies (Fig. 1 A) when compared with age-matched controls (Fig. 1 B). Skeletal lesions increased in severity with age (Fig. 2 A, B) and were most apparent in the lumbar spinal column. Changes included a reduction in vertebral size, retarded ossification, increased intervertebral disk spaces, and irregular vertebral epiphyses (Figs. 1 A, 2 A). Similar abnormalities were noted in the vertebral column of the affected child (Fig. 3).

Longitudinal sections through the vertebral column in affected dogs and child confirmed the radiographic findings of abnormally widened intervertebral disk spaces and abnormal vertebral epiphyses.

Histological, histochemical and ultrastructural findings

In affected dogs, histological examination revealed retarded endochondral ossification at vertebral epiphyses. This observation was best demonstrated with sections stained with safranin-O. At 2 months of age, about two-thirds of an epiphysis was ossified in normal puppies (Fig. 4 A). In contrast, in affected puppies less than half was ossified (Fig. 4 B). At 9 months of age ossification of the vertebral epiphyses in normal puppies was complete (Figs. 5 A, 7 A) but not in affected puppies (Figs. 5 B, 7 B). At 2 months of age, the growth plates from normal puppies had a well developed primary spongiosa (Fig. 6 A). In age-matched affected puppies, the primary spongiosa was poorly developed, and there was metaphyseal osteoporosis (Fig.6 B). It is noteworthy that at 9 months of age focal physeal cartilage necrosis was observed only in affected puppies (Fig.7 B, C). Similarly, retarded ossification at vertebral epiphyses, poorly developed primary spongiosa and metaphyseal osteoporosis

Table 1 Lectins used for identifying carbohydrate residues (*Gal* galactose, *GalNAc* N-acetylgalactosamine, *Glc* glucose, *Man* mannose, *GlcNAc* N-acetylglucosamine, *NeuNAc* N-acetylneuraminic acid sialic acid)

Lectin origin	Common name	Acronym	Concentration (μg/ml)	Major sugar specification	Binding inhibitor
Arachis hypogea	Peanut	PNA	20	Gal-β-(1-3)-GalNAc	Lactose
Concanavalia ensiformis	Jack bean	Con A	10	α-D-Glc, α-D-Man	α-D-methyl-Man
Datura stramonium	Jimsonweed	DSA	10	$[\beta\text{-D-Gal-(1}\rightarrow\text{4)-}\beta\text{-D-GlcNAc-(1}\rightarrow\text{3)}]_n$	$(\beta\text{-D-GlcNAc})_{2-3}$
Dolichos biflorus	Horse gram	DBA	10	α-D-GalNAc	α-D-GalNAc
Glycine max	Soybean	SBA	10	α-D-GalNAc, α-D-Gal	α-D-GalNAc
Griffonia simplicifolia	Bandeirea	GS-I	50	α-D-Gal	Lactose
Lens culinars	Common lentil	LCA	10	α-D-Glc, α-D-Man	α-D-methyl-Man
Ricinus communis	Castor bean	RCA-I	50	β-D-Gal	Lactose
Triticum vulgaris	Wheatgerm	WGA	50	$[\beta\text{-(1}\rightarrow\text{4)-D-GalNac)}_2$, NeuNAc	NeuNAc
	Succinyl-WGA	S-WGA	10	$[\beta\text{-(1}\rightarrow\text{4)-D-GlcNAc]}_2$	β-D-GlcNAc
Ulex europaeus	Gorse	UEA-I	10	α-L-fucose	α-L-fucose

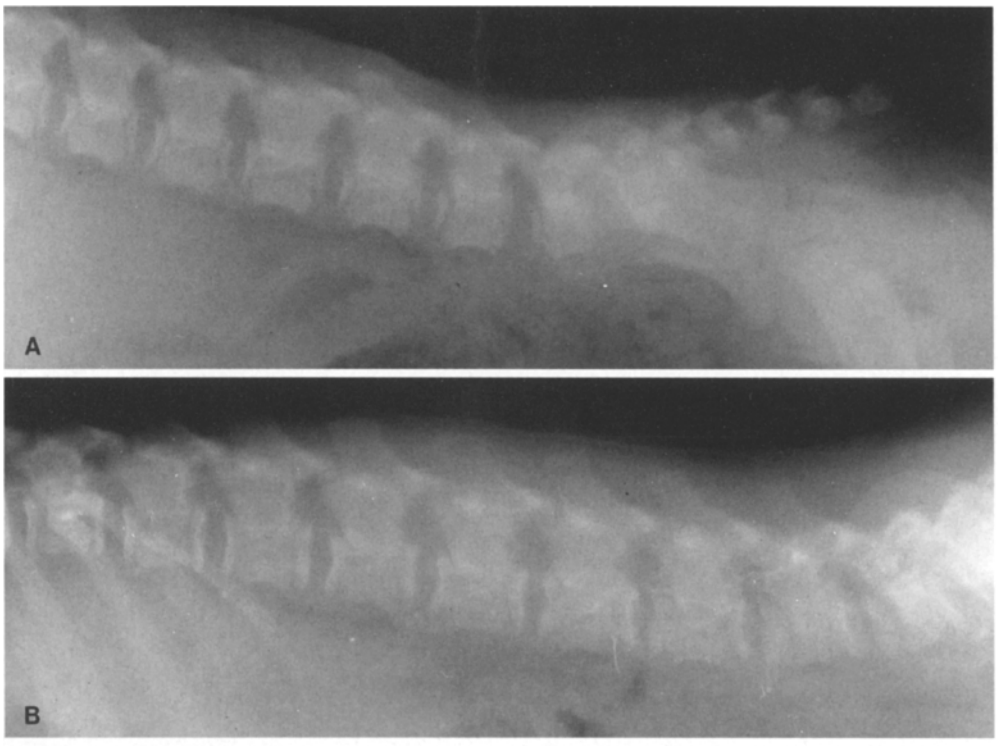

Fig. 1 Lateral radiographs of the lumbar vertebrae of a 2-month-old affected puppy (**A**) and his normal Portuguese water dog (PWD) brother (**B**). The ossified physes of the affected puppy are short and irregular

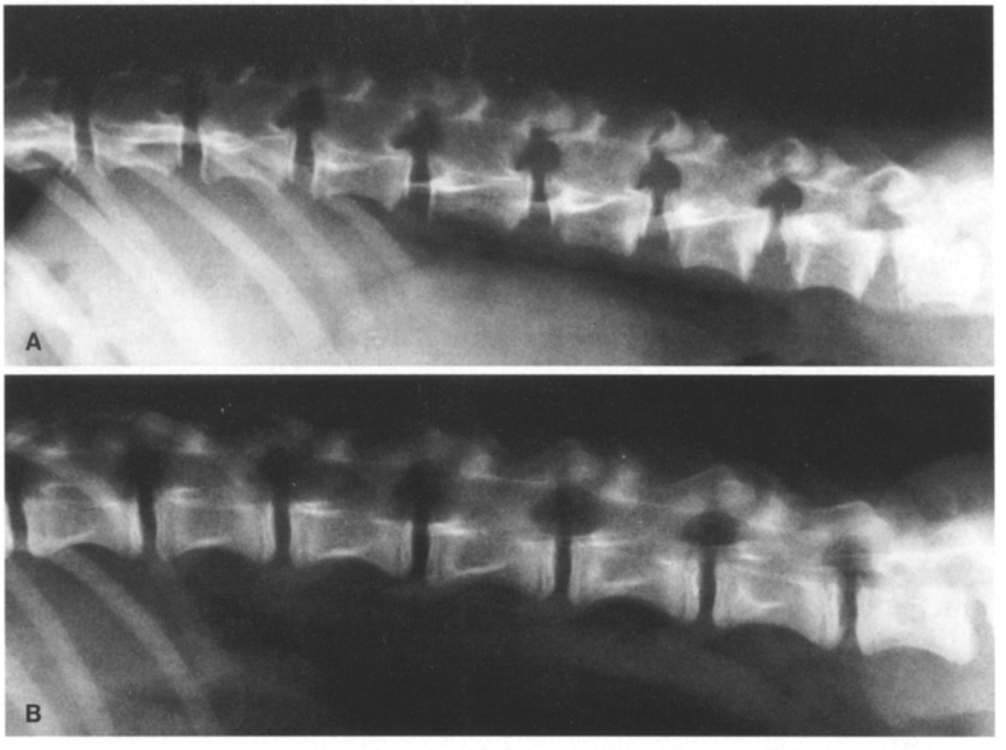

Fig. 2 Lateral radiographs of lumbar vertebrae of a 9-month-old normal English springer spaniel (ESS) puppy (**B**) and his affected brother (**A**). In **A** the vertebrae are shorter and the intervertebral disks are irregular and wide

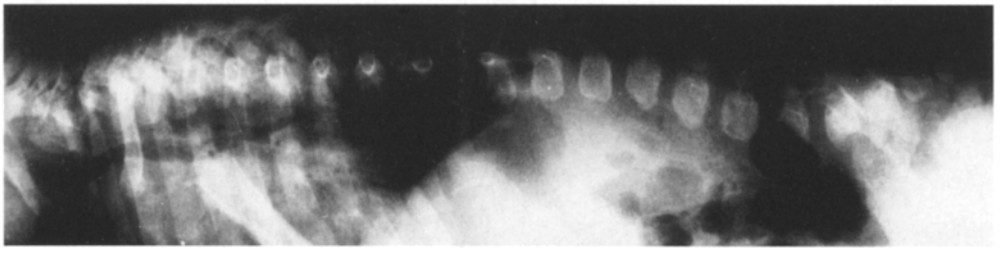

Fig. 3 Lateral radiograph of the vertebral column of a 4 1/2-month-old child with G_{M1}-gangliosidosis. The lumbar vertebrae are irregular and the intervertebral disks are wide

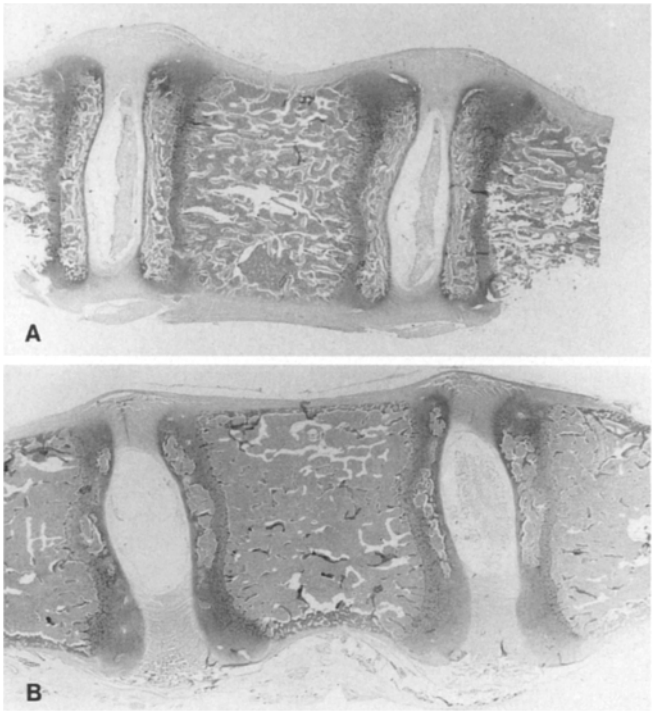

Fig. 4 Longitudinal section through the lumbar vertebrae and intervertebral disks of a 2-month-old normal PWD (**A**) and his affected sex and age-matched brother (**B**), safranin O, ×4. **A** In normal puppy two-thirds of the physics is ossified. **B** In the affected puppy less than half is ossified and there is metaphyseal osteoporosis

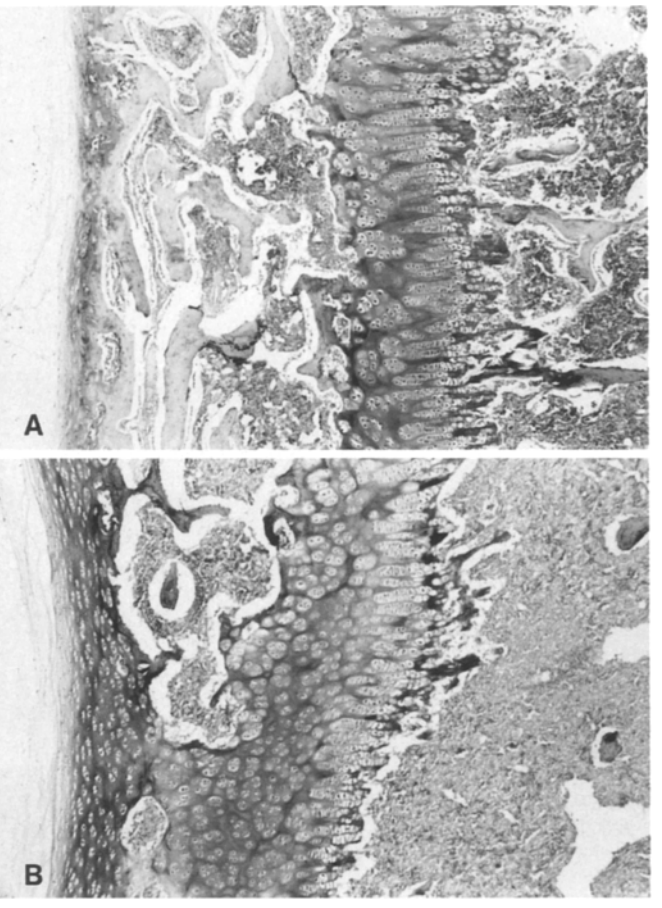

Fig. 6A, B Closer view of the physes seen in Figure 4 A, B, safranin O, ×35. **A** In the normal puppy the ossification is advanced and the primary spongiosa are well developed. **B** In the affected puppy the ossification is retarded, the primary spongiosa are poorly developed and there is metaphyseal osteoporosis

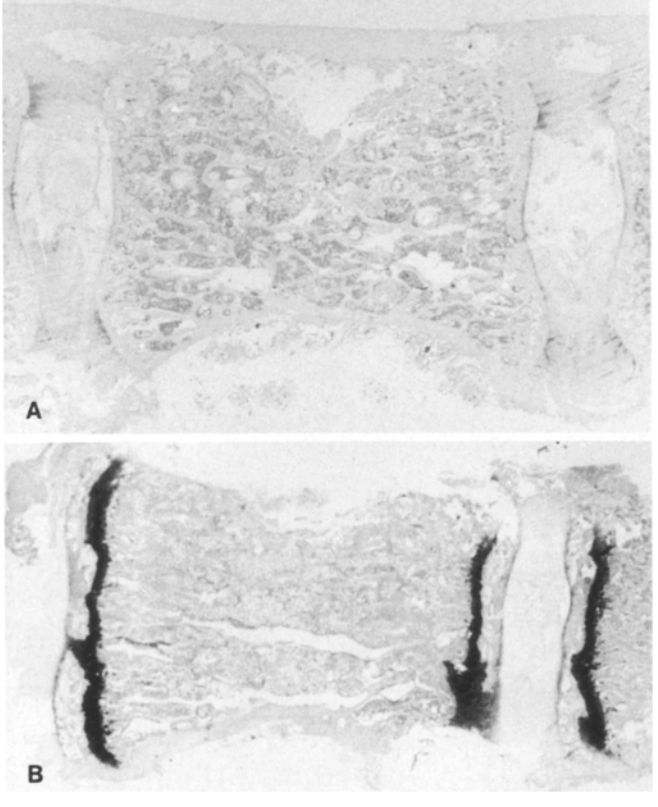

Fig. 5 Longitudinal section through a lumbar vertebra and and intervertebral disks of a 9-month-old normal ESS (**A**) and his sex and age-matched, affected brother (**B**), safranin O, ×5. **A** The vertebra of the normal puppy is larger than his affected brother (**B**) and contains numerous bone spicules. The physes, however, did not stain positively with safranin O. **B** The vertebra of the affected puppy is smaller and contains fewer bone spicules and the growth plates stained intensely with safranin O. These findings indicate retarded bone formation with retained cartilage in the affected puppy

(Fig.8) were noted in the affected 15-month-old child. Chondrocytes from affected puppies and the affected child were enlarged and vacuolated. This observation was best demonstrated in 1 μm thick, toluidine blue stained sections (Fig. 9). In addition, the osteoblasts, osteoclasts and osteocytes were vacuolated (Fig. 10).

There were only minor differences in the staining intensity with lectin reagents and for S-100 protein in chondrocytes from affected and age-matched control puppies. Chondrocytes of control and affected puppies and the affected child stained with 3 of 11 lectins (Con A, RCA-I and WGA), and the staining intensity was

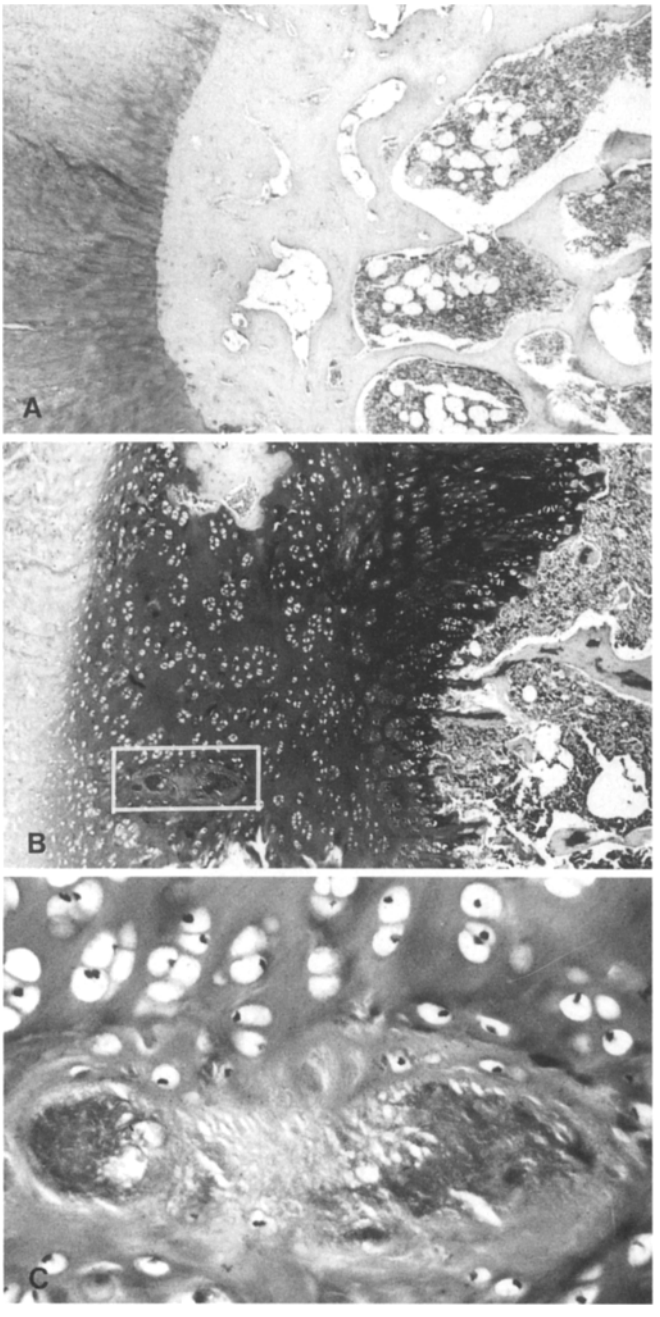

Fig. 7A–C Closer view of the physes seen in Figure 5 A, B, safranin O, ×37. **A** The normal puppy shows complete ossification. **B** The affected puppy shows retained cartilage with grouping of chondrocytes, necrotic foci, poorly developed primary spongiosa and narrowed bone spicules. **C** High magnification of the cartilage in the rectangle in **B** illustrating the necrotic cartilage and vacuolated chondrocytes, safranin O, ×240

greater in the affected puppies (Fig. 11). Furthermore, some of the chondrocytes in the affected puppies stained moderately with PNA. Unlike the observation cited in a previous report [14], chondrocytes from normal and affected puppies and the affected child did not stain with neuron specific enolase. Cytoplasmic staining for S-100 protein in chondrocytes from affected puppies and the

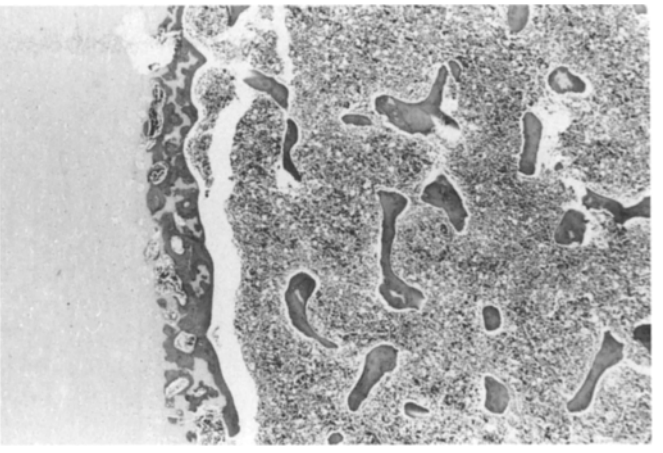

Fig. 8 Lumbar vertebral metaphysis from a 15-month-old child with G_{M1}-gangliosidosis illustrating osteoporosis. Haematoxylin and eosin (H & E), ×35

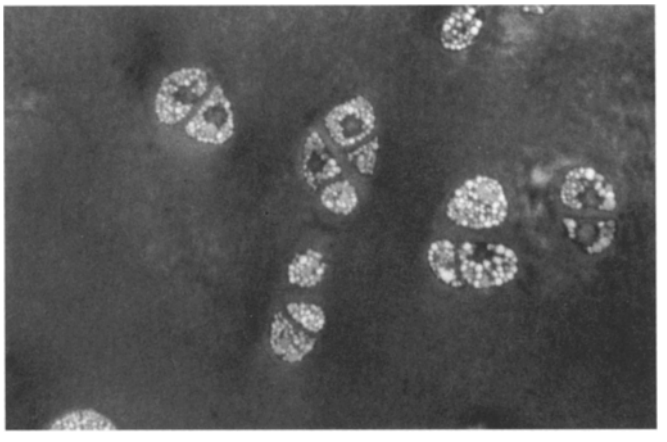

Fig. 9 One micron section through costochondral junction from an 8-month-old PWD. Most of the chondrocytes are vacuolated. Toluidine blue, ×550

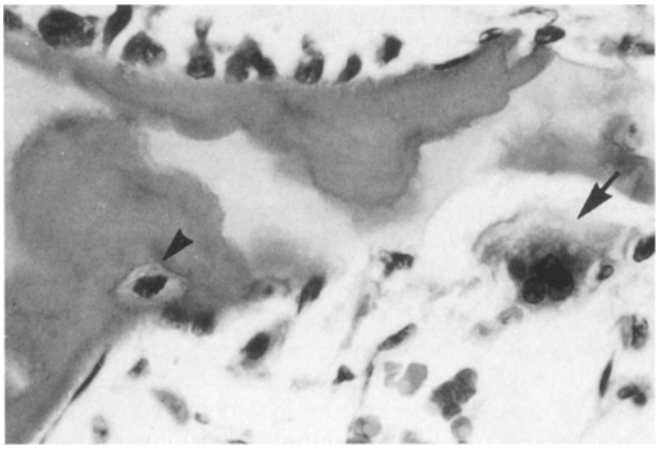

Fig. 10 Section through femur of a 15-month-old child with G_{M1}-gangliosidosis showing vacuolated osteocyte (*arrowhead*) and osteoclast (*arrow*). H & E, ×580

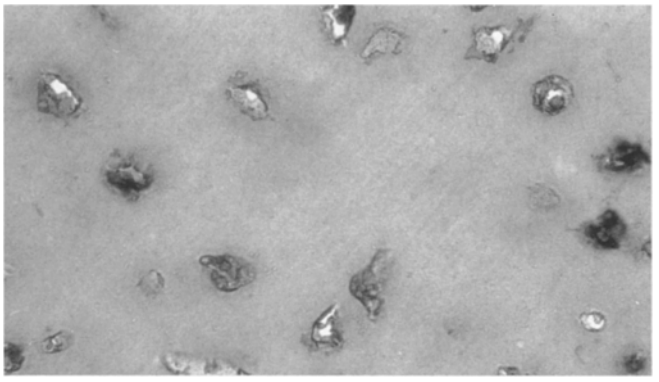

Fig. 11 Section through costochondral junction from the affected child demonstrate staining of the chondrocytes with RCA-I, ×350

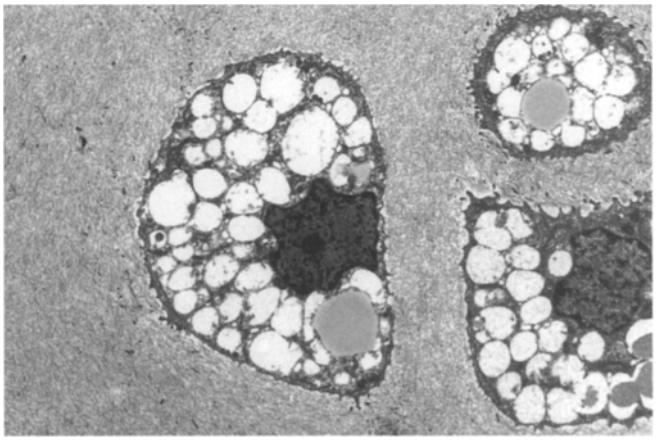

Fig. 12 Electron micrograph of three chondrocytes in the rib cartilage from an 8-month-old affected dog. The chondrocytes are vacuolated and contain lipid droplets. ×3700

child was intense but patchy; by comparison, the staining in control dogs was diffuse but weaker.

Ultrastructurally, chondrocytes in affected puppies (Figs. 12) and the affected child (Fig. 13) contained large vacuoles (secondary lysosomes) laden with small fine fibrils and infrequent lamellated membrane structures. The characteristically distended cisternae of rough endoplasmic reticulum were displaced and narrowed (Fig. 13).

Discussion

Some human and animal lysosomal storage diseases are associated with skeletal lesions [1, 5, 10, 11, 12, 23, 24, 34]. Most of the information on skeletal abnormalities in these disorders is found in the radiological literature. In many of these disorders the radiographic findings are relatively distinct and are useful in establishing a diagnosis [20, 29, 33]. There are only limited morphological descriptions of either cartilaginous or bony lesions from case reports of individuals afflicted with these disorders

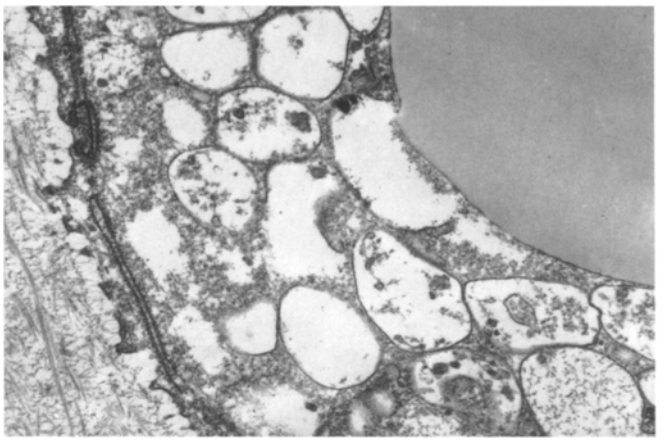

Fig. 13 Higher magnification of a rib chondrocyte from an affected 15-month-old child. The secondary lysosomes contain fine fibrils and membrane fragments. The cisternae of the rough endoplasmic reticulum are narrow and displaced to the chondrocyte periphery. ×16 900

[17, 27, 28, 31]. In the current study we used radiological, morphological and histochemical methods to characterize the development of skeletal lesions in two different animal models of G_{M1}-gangliosidosis [3] and in a child with the infantile form of G_{M1}-gangliosidosis. We described the presence of storage material-laden chondrocytic lysosomes that stained intensely with Con A, WGA and RCA-I. These observations suggest that a partially degraded compound/s with α-mannosyl, β-N-acetylglucosaminyl and/or sialyl and β-galactosyl residues, respectively, has accumulated [3], a finding that is in accord with the sugar residues found in keratan sulfate and oligosaccharides which are stored in G_{M1}-gangliosidosis [24]. Furthermore, we demonstrated abnormal endochondral ossification and metaphyseal osteoporosis in both canine models of G_{M1}-gangliosidosis and in a child with the infantile form of the disease. In addition, we observed focal cartilage necrosis in the 9-month-old affected puppies, a similar lesion previously noted in the lumbar vertebrae of a 1-year-old cat with MPS-VI [26].

Despite the paucity of data regarding the pathogenesis of skeletal lesions in the lysosomal storage diseases, preexistent radiological and limited morphological data suggest that multiple mechanisms are involved. At least two distinct pathological processes are believed to contribute to the development of the skeletal lesions. The first process involves the accumulation of lipid-laden reticuloendothelial cells within the medullary cavity leading to "pressure atrophy" of the primary and secondary spongiosa, or chronic ischaemia with resultant focal necrosis, osteoporosis and pathological fractures of long bones or collapse of vertebral bodies. Such lesions are observed in Gaucher's disease and, to a lesser extent, in Niemann-Pick disease [4, 32, 34].

In contrast, the lesions observed in lysosomal disorders with storage of mucopolysaccharides and oligosaccharides and in the mucolipidoses are probably due to abnormal cartilage and bone formation [17, 27, 28, 31].

Cartilage and bone are developmentally linked in that most of the bones of the skeleton are formed via a cartilage anlage. Endochondral ossification is the pathway by which bones of the vertebral column and appendicular skeleton are formed and grow in length. Cartilage is composed of sparsely distributed chondrocytes which may comprise as little as 10% of the total volume. They are embedded in an extracellular matrix that consists of a highly concentrated gel of proteoglycan immobilized within a dense network of collagen fibrils [7] and other non-collagenous macromolecules [13]. Cartilage proteoglycan is a high molecular weight molecule that consists of a large number of carbohydrate chains that account for up to 90% of its total weight. The carbohydrate chains contain glycosaminoglycans composed on chondroitin 4-sulfate, chondroitin 6-sulfate and keratan sulfate, as well as N- and O-linked oligosaccharide chains [7]. Collagen types II, IX (which contains a proteoglycan moiety), X and XI are found almost exclusively in cartilage [19]. In the maturing physis there is a progressive increase in the activity of lysosomal enzymes [8] and progressive loss of the proteoglycan as the volume of the extracellular matrix is reduced [18]. It is possible that retarded bone formation in G_{M1}-gangliosidosis, a condition in which there is deficient activity of lysosomal β-galactosidase, may be attributable to accumulation of undegraded β-galactosyl-containing carbohydrate chains of proteoglycan units. Conversely it is possible that inhibition of glycosaminoglycan degradation by lysosomal hydrolases may result in reduced glycosaminoglycan synthesis. The latter possibility is supported by recent findings in which inhibition of lysosomal function with lysosomotropic amine resulted in reduced degradation and synthesis of glycosaminoglycans [6, 16].

The properties which enable cartilage to withstand large compressive forces are the viscoelastic gel of polyanionic proteoglycans and the firmness of the interlacing network of collagen [7]. Thus, the abnormal composition of cartilage proteoglycans found in the lysosomal storage diseases, such as MPS and mucolipidoses, may contribute to the observed skeletal lesions [25]. It is well documented that small proteoglycans may inhibit the fibrillogenesis of type II collagen [35], which is the major collagen of cartilage [19]. Similar interaction between proteoglycans and collagen was described in the skin of patients with aspartylglycosaminuria [21, 22]. Structural changes of collagen were attributed to abnormal proteoglycan in aspartylglycosaminuria, a lysosomal disease with storage of partially degraded N-linked oligosaccharides [21, 22]. A similar abnormality of collagen might lead to loss of firmness of cartilage resulting in focal necrosis as seen in the vertebrae of our 9-month-old affected puppies and a cat with MPS-VI [1, 26].

In conclusion, the development of skeletal lesions in human and canine G_{M1}-gangliosidosis has been described. Furthermore, we have discussed the possible role of the extracellular matrix in the development of these lesions.

Acknowledgements We thank Mrs. Vibha Goyal for her technical assistance and Mrs. Elizabeth Smith for her aid with the manuscript.

References

1. Alroy J, Lee RE (in press) The pathology of the skeleton in lysosomal storage diseases. In: Rosenberg AE, Schiller AL (eds) Orthopaedic pathology. WB Saunders, Philadelphia
2. Alroy J, Warren CD, Raghavan SS, Kolodny EH (1989) Animal models for lysosomal storage diseases: their past and future contribution. Hum Pathol 20:823–826
3. Alroy J, Orgad U, DeGasperi R, Richard R, Warren CD, Knowles K, Thalhammer JG, Raghavan SS (1992) Canine G_{M1}-gangliosidosis: a clinical, morphological, histochemical and biochemical comparison of two models. Am J Pathol 140:675–689
4. Barranger JA, Ginns EI (1989) Glucosylceramide lipidoses: Gaucher's disease. In: Scriver CR, Beaudet AL, Sly WS, Valle D (eds) The metabolic basis of inherited disease, 6th edn. McGraw-Hill, New York, pp 1677–1698
5. Beaudet AL, Thomas GH (1989) Disorders of glycoprotein degradation: mannosidosis, fucosidosis, sialidosis and aspartylglucosaminoria. In: Scriver CR, Beaudet AL, Sly WS, Valle D (eds) The metabolic basis of inherited disease, 6th edn. McGraw-Hill, New York, pp 1603–1621
6. Carinci P, Looci P, Evangelisti R, Marinucci L, Rossi L, Becchetti E (1991) Relation between hyaluronan and sulphated glycosaminoglycan synthesis and degradation in cultured embryonic fibroblasts. Effect of Concanavalin A and ammonium chloride administration. Cell Biochem Funct 9:255–262
7. Carney SL, Muir H (1988) The structure and function of cartilage proteoglycans. Physiol Res 68:858–910
8. deKleer VS (1982) Development of bone. In: Summer-Smith G (ed) Bone in clinical orthopaedics: a study in comparative osteology. WB Saunders, Philadelphia, pp 1–80
9. Gamble JG, Haimson R, Smith RL (1990) Glucosaminidase, galactosaminidase, and glucuronidase in growth plate. J Orthop Res 8:764–768
10. Haskins ME, Aguirre GD, Jezyk PF, Patterson DF (1980) The pathology of the feline model of mucopolysaccharidosis VI. Am J Pathol 101:657–674
11. Haskins ME, Aguirre GD, Jezyk PF, Desnick RJ, Patterson DF (1983) The pathology of feline model of mucopolysaccharidosis I. Am J Pathol 112:27–36
12. Haskins ME, Desnick RJ, DiFerrante N, Jezyk PF, Patterson DF (1984) β-glucuronidase deficiency in a dog: a model of human mucopolysaccharidosis VII. Pediatr Res 18:980–984
13. Heinegard D, Oldberg A (1989) Structure and biology of cartilage bone and bone matrix noncollagenous macromolecules. FASEB J 3:2042–2051
14. Karabela-Bouropoulou V, Markaki S, Milas CH (1988) S-100 protein and neuron specific enolase immunoreactivity of normal, hyperplastic and neoplastic chondrocytes in relation to the composition of extracellular matrix. Pathol Res Pract 183:761–766
15. Konde LJ, Thrall MA, Gasper P, Dial SM, McBiles K, Colgan S, Haskins M (1987) Radiographically visualized skeletal changes associated with mucopolysaccharidosis VI in cats. Vet Radiol 28:223–228
16. Locci P, Evangelisti R, Lilli C, Stabellini G, Becchetti E, Carinci P (1992) An evaluation of the mechanisms developmentally involved on cellular and extracellular glycosaminoglycans accumulation in chick embryo skin fibroblasts. Int J Biochem 24:151–158
17. Martin JJ, Leroy JG, Farriaux JP, Fontaine G, Desnick RJ, Cabello A (1975) I-cell disease (mucolipidosis II): a report on its pathology. Acta Neuropath (Berl) 33:285–305
18. Matsui Y, Alini M, Webber C, Poole R (1991) Characterization of aggregating proteoglycans from the proliferative, ma-

turing, hypertrophic, and calcifying zones of the cartilagenous physis. J Bone Joint Surg [Am] 73:1064–1074
19. Mayne R (1989) Cartilage collagens: what is their function, and are they involved in articular disease. Arthritis Rheum 32:241–246
20. Milgram JW (1990) Radiologic and histologic pathology of nontumorous diseases of bones and joints (vol. 1). Northbrook Publishing, Northbrook, pp 131–148
21. Nanto-Salonen K, Pelliniemi LJ, Autio S, Kivimaki T, Rapola J, Penttinen (1984) Abnormal collagen fibrils in aspartlyglycosaminuria: altered dermal ultrastructure in a glycoprotein storage disorder. Lab Invest 51:464–468
22. Nanto-Salonen K, Larjava H, Saamanen AM, Heino J, Penttinen R, Pelliniemi LJ, Tammi M (1987) Abnormal dermal proteoglycan in aspartylglycosaminuria: a possible mechanism for ultrastructural changes of collagen fibrils in a glycoprotein storage disorder. Conn Tissue Res 16:367–376
23. Neufeld EF, Muenzer J (1989) The mucopolysaccharidoses. In: Scriver CR, Beaudet AL, Sly WS, Valle D (eds) The metabolic basis of inherited disease, 6th edn. McGraw-Hill, New York, pp 1565–1587
24. O'Brien JS (1989) β-galactosidase deficiency (G_{M1}-gangliosidosis, galactosialidosis, and Morquio syndrome type B); ganglioside sialidase deficiency (mucolipidosis IV). In: Scriver CR, Beaudet AL, Sly WS, Valle D (eds) The metabolic basis of inherited disease, 6th edn. McGraw-Hill, New York, pp 1797–1806
25. Oohira A, Matsui F, Nogami H (1986) Aberrant composition of chondroitin sulfates in cartilae-type proteoglycan isolated from iliac crest of patients with some lysosomal storage diseases. J Biochem (Tokyo) 99:1371–1376
26. Orgad U, Schelling S, Alroy J, Rosenberg A, Schiller A (1989) Skeletal lesions in lysosomal storage disease (abstract). Lab Invest 60:406
27. Pazzaglia UE, Beluffi G, Bianchi E, Castello A, Coci A, Marchi A (1989) Study of the bone pathology in early mucopolipidosis II (I-cell disease). Eur J Pediatr 148:553–557
28. Rabinowitz JG, Sacher M (1974) Gangliosidosis (G_{M1}): a reevaluation of vertebral deformity. Am J Roentgenol 121:155–158
29. Resnick D, Niwayama G (1988) Diagnosis of bone and joint disorders, 2nd edn (vol. 5). WB Saunders, Philadelphia, pp 3501–3515
30. Roberts DJ, Ampola MG, Lage JM (1991) Diagnosis of unsuspected fetal metabolic storage by routine placental examination. Pediatr Pathol 11:647–656
31. Schenk EA, Haggerty J (1964) Morquio's disease: a radiologic and morphologic study. Pediatrics 34:839–850
32. Spence MW, Callahan JW (1989) Sphingomyelin-cholesterol lipidoses: the Niemann-Pick group of diseases. In: Scriver CR, Beaudet AL, Sly WS, Valle D (eds) The metabolic basis of inherited disease, 6th edn. McGraw-Hill, New York, pp 1655–1676
33. Spranger JW, Langer LO, Weidmann H-R (1974) Bone dysplasias: an atlas of constitutional disorders of skeletal development. WB Sanders, Philadelphia, pp 143–187
34. Stowens DW, Teitelbaum SL, Kahn AJ, Barranger JA (1985) Skeletal complications of Gaucher's disease. Medicine (Baltimore) 64:310–322
35. Vogel KG, Paulsson M, Heinegard D (1984) Specific inhibition of type I and type II collagen fibrillogenesis by small proteoglycan of tendon. Biochem J 223:587–597
36. Vogler C, Brikenmeier EH, Sly SW, Levy B, Pegors C, Kyle JW, Beamer WG (1990) A murine model of mucopolysaccharidosis VII. Gross and microscopic findings in beta-glucuronidase-deficient mice. Am J Pathol 136:207–217